Article

Journal of
Nanoscience and Nanotechnology
Vol. 14, 6539–6550, 2014
www.aspbs.com/jnn

Simultaneous Determination of Ascorbic Acid, Dopamine, Uric Acid, and Tryptophan by Nanocrystalline ZSM-5 Modified Electrodes

Balwinder Kaur and Rajendra Srivastava*

Department of Chemistry, Indian Institute of Technology Ropar, Rupnagar 140001, Punjab, India

Nanocrystalline ZSM-5 was prepared by using propyltriethoxysilane as an additive in the conventional ZSM-5 synthesis composition. Materials were characterized by a complementary combination of X-ray diffraction, nitrogen sorption, and Scanning electron microscopy. Transition metal ion exchanged nanocrystalline ZSM-5 (M-Nano-ZSM-5, where M = Cu^{2+}, Ni^{2+}, Co^{2+}, Fe^{2+}, and Mn^{2+}) modified electrodes were constructed for the simultaneous determination of ascorbic acid (AA), dopamine (DA), uric acid (UA), and tryptophan (Trp). Electrochemical studies were carried out by using cyclic voltammetry, linear sweep voltammetry, and chronoamperometry in buffer solution at pH 3.5. Fe-Nano-ZSM-5 modified electrode exhibited excellent electrocatalytic activity with well-separated oxidation peaks towards AA, DA, UA, and Trp in their simultaneous determination. Among the M-Nano-ZSM-5 and transition metal ion-exchanged ZSM-5 (M-ZSM-5) materials investigated in this study, Fe-Nano-ZSM-5 exhibited the highest catalytic activities towards the oxidation of AA, DA, UA, and Trp with good stability, sensitivity, and selectivity. The analytical performance of this sensor was demonstrated for the simultaneous determination of AA, DA, UA, and Trp in blood serum and UA concentration in urine samples.

Keywords: Nanocrystalline ZSM-5, Ion-Exchange, Simultaneous Determination, Electrocatalytic Oxidation, Bio-Molecules.

1. INTRODUCTION

Medical scientists have made significant contribution to understand the chemistry of human body. The deficiency or maladjustment of various bio-molecules present in body may lead to many diseases. Thousands of different bio-molecules exist in the body and it is almost impossible to detect them in one run, because of their different chemical properties. It would be very interesting if we can detect at least a class of compounds in one run, then it is a great achievement in the medical science. In this study, nanocrystalline zeolite based modified electrodes were constructed and find their potential application as electrochemical sensor in the simultaneous detection of four different physiologically important bio-molecules.

Tryptophan (Trp) is an essential amino acid required for the biosynthesis of proteins (precursor molecules of hormones, neurotransmitters and other relevant bio-molecules) and find importance in nitrogen balance and the maintenance of muscle mass and body weight in humans.[1] To correct possible dietary deficiencies, Trp is added to dietary and food products as a food fortifier and to pharmaceutical formulations. HPLC and spectrophotometric procedures are known to determine the Trp concentration; however these methods are complex and time consuming.[2] Uric acid (UA) is the end product of purine metabolism and its concentration in the body should be maintained.[3] Its abnormal concentration level leads to several diseases such as hyperuricemia, gout, leukemia, and pneumonia.[4] Dopamine (DA) is an important neurotransmitter in the mammalian central nervous system.[5] Low levels of DA may cause neurological disorders such as schizophrenia and Parkinson's disease.[6] Ascorbic acid (AA) prevents scurvy and is known to take part in several biological reactions. It has been widely used in foods and drinks as an antioxidant and also for the prevention and treatment of common cold, mental illness, infertility, cancer, and AIDS.[7] AA, DA, UA, and Trp usually coexist in blood serum. Therefore, the development of a

*Author to whom correspondence should be addressed.

sensitive and selective method for their simultaneous determination is highly desirable for analytical application and diagnostic research. AA, DA, UA, and Trp are electrochemically active and therefore, in principle, it is possible to detect them simultaneously using electrochemical method. However, it was found that they are oxidized at nearly the same potential with poor sensitivity at unmodified electrodes.[8] To overcome this problem, various modified electrodes have been constructed and investigated in their simultaneous determination.[9(a)–(d)] These modified electrodes are successful in detecting either two or three such species simultaneously.[10(a)–(f)] Simultaneous detection of all four species is rarely reported.[11] Very recently, we have reported the simultaneous determination of AA, DA, UA, and Trp using transition metal exchanged mesoporous polyaniline.[12]

Microporous crystalline aluminosilicate, zeolites, are widely used as shape-selective catalysts, ion-exchanged materials, and adsorbents for organic compounds.[13] Adsorptive and ion-exchange properties of zeolite were explored for obtaining modified electrodes.[14] Their superior performance can often be attributed to the existence of a well-defined system of micropores (size below 1.5 nm in diameter) with uniform shape and size, typically of molecular dimensions. However, for some applications, the presence of such micropores alone can also result in an unacceptably slow diffusion of reactants and products to and from the active sites located inside the zeolite crystals.[15] To overcome this diffusion limitation, two approaches have been adopted; either to minimize the crystal size of zeolite catalysts (nanocrystalline zeolite) or prepare a zeolite with interconnected micropores and mesopores (hierarchical zeolite).[16] In recent years, zeolites with interconnected intra- or inter-crystalline mesoporosity have attracted much attention due to improved diffusion, catalytic activity, selectivity, and retardation against deactivation.[17, 18] Several attempts have been made for the preparation of nanosized zeolites.[19, 20(a)–(d)] There are only a few reports available in literature, where zeolites modified electrodes have been used for the detection of biological compounds.[21(a), (b)] In this study, transition metal exchanged nanocrystalline ZSM-5 (M-Nano-ZSM-5 where $M = Cu^{2+}$, Ni^{2+}, Co^{2+}, Fe^{2+}, and Mn^{2+}) based electrodes were constructed for the detection of AA, DA, UA, and Trp and results are compared with the transition metal exchanged ZSM-5 (M-ZSM-5) based electrodes.

2. EXPERIMENTAL DETAILS

2.1. Chemicals

All chemicals used in the study were of A.R. grade and used as received without further purification. Tetraethylorthosilicate (TEOS), propyltriethoxysilane (PrTES), and tetrapropylammonium hydroxide (TPAOH) were purchased from Aldrich. $CuCl_2 \cdot 2H_2O$, $MnCl_2 \cdot 4H_2O$, $NiCl_2 \cdot 6H_2O$, $CoCl_2 \cdot 6H_2O$, $FeCl_2 \cdot 4H_2O$, D-(+)-Glucose, and NaOH were obtained from Spectrochem Pvt. Ltd., whereas dopamine, L-ascorbic acid, uric acid, and tryptophan were obtained from Himedia Pvt. Ltd. The standard phosphate buffer solutions with different pH values were prepared by adding 7.5 M aqueous NaOH solution to aqueous solution of ortho phosphoric acid [$H_3PO_4 = 10.11$ mL (85% aqueous solution) in 1 L of aqueous solution] while magnetically stirring until the pH of the aqueous solution reached the desired value (1.0, 3.5, 5.0, 7.0, and 9.0). The electrochemical measurements were performed in buffer solution (pH 3.5). Deionized water from Millipore Milli-Q system (Resistivity 18 MΩcm) was used in the electrochemical studies. Blood serum samples and urine samples were obtained from Parmar Hospital, Ropar, Punjab, India.

2.2. Sample Preparation

Nano-ZSM-5 was synthesized by following the reported procedure.[19] In a typical synthesis, 1.2 g of sodium aluminate (53 wt.% Al_2O_3, 43 wt.% Na_2O) was dissolved in 25 mL of distilled water (Solution A). 2.06 g of PrTES was mixed with 25 mL of TPAOH (1 M aq. solution) (Solution B). Solution A and solution B were mixed, and the resultant solution was stirred for 15 minutes at ambient condition, until it became a clear solution. 18.7 g of TEOS was added into the resultant solution and stirring was continued for 6 h. The molar composition of the gel mixture was 90 TEOS/10 PrTES/2.5 Al_2O_3/3.3 Na_2O/25 TPAOH/2500 H_2O. This mixture was transferred to a Teflon-lined autoclave, and hydrothermally treated at 443 K for 3 days under static conditions. The final product was filtered, washed with distilled water and dried at 373 K. Material was calcined at 823 K for 4 h under flowing air. ZSM-5 was synthesized at 443 K using the same synthesis composition as mentioned above for the Nano-ZSM-5, but without PrTES additive. Nano-ZSM-5 and ZSM-5 (1 g) were cation exchanged into M-Nano-ZSM-5 or M-ZSM-5 (where M = Cu, Ni, Co, Mn, Fe) by repeating the ion-exchange, three times with a 50 mL of 1 M aqueous solution of metal source at 343 K for 4 h. Metal contents were obtained using the atomic absorption spectrophotometer (AAS).

2.3. Electrode Fabrication

Cyclic voltammetry (CV), linear sweep voltammetry (LSV) and chronoamperometric studies of zeolite samples were performed using Potentiostat-Galvanostat BASi EPSILON, USA. A three electrode electrochemical cell was employed with Ag/AgCl as the reference electrode (3 M KCl), zeolites mounted glassy carbon (3 mm diameter) as the working electrode, and Pt foil as the counter electrode. Before modification, the polished electrode was ultrasonicated in ethanol and deionized water for 5 minutes, respectively. 20 μL aliquot of zeolite suspension (a homogenous sonicated solution of 2 mg of zeolite, 10 μL nafion, and 1 mL of deionized water) was placed onto the electrode surface, the

electrode was dried in air leaving the material mounted onto the glassy carbon surface.

2.4. Characterization

X-ray diffraction (XRD) patterns were recorded in the range of 5–80° on a PANalytical X'PERT PRO diffractometer using Cu Kα radiation ($\lambda = 0.1542$ nm, 40 kV, 20 mA) and a proportional counter detector. Nitrogen adsorption measurement at 77 K was performed by Autosorb-IQ Quantachrome Instruments volumetric adsorption analyzer. Samples were out-gassed at 573 K for 2 h in the degas port of the adsorption apparatus. The specific surface area was determined by BET method using the data points of P/P_0 in the range of about 0.05–0.3. The pore diameter was estimated using the Barret–Joyner–Halenda (BJH) model. Scanning electron microscopy (SEM) measurements were carried out on a JEOL JSM-6610LV to investigate the morphology of the materials. During the SEM investigation, energy-dispersive X-ray spectroscopy (EDS) was utilized in the sample characterization and the EDS elemental maps were obtained. The chemical composition of the samples was estimated by atomic absorption spectrophotometer (Analytic Jena Model AAS 5EA, Germany).

3. RESULTS AND DISCUSSION

3.1. Physicochemical Characterizations

Nano-ZSM-5 exhibited MFI framework structure with high phase purity, which was confirmed by using XRD (Fig. 1(a)). The XRD pattern of Nano-ZSM-5 is broad in nature, confirming the nanocrystalline nature of the material. M-Nano-ZSM-5 and M-ZSM-5 also exhibited XRD pattern corresponding to a highly crystalline MFI structure. The N_2-adsoption isotherm for Nano-ZSM-5 showed a type-IV isotherm similar to the mesoporous silica materials (Fig. 1(b)). The major difference in the isotherm of Nano-ZSM-5 when compared to ZSM-5 is a distinct increase of N_2 adsorption in the region $0.4 < P/Po < 0.95$, which is interpreted as capillary condensation in mesopore void spaces. The mesopores show a pore size distribution in the range of 1–10 nm. Surface area and pore volume of M-Nano-ZSM-5 and M-ZSM-5 were found to be similar when compared to Nano-ZSM-5 and ZSM-5, respectively (Table I). The SEM images show that the spheroid shaped Nano-ZSM-5 particles are composed of very small nanocrystals (Fig. 2(a)). Zeolite particles with capsule-like

Table I. Physico-chemical characteristics of zeolites investigated in this study.

Sample	Transition metal content in zeolite (mg/g)	Total surface area (m^2/g)	External surface area (m^2/g)	Total pore volume (cm^3/g)
ZSM-5	–	286	50	0.201
Nano-ZSM-5	–	492	246	0.412
Cu-Nano-ZSM-5	123.8	476	234	0.400
Ni-Nano-ZSM-5	123.2	483	240	0.407
Co-Nano-ZSM-5	119.0	475	237	0.400
Fe-Nano-ZSM-5	114.5	480	243	0.405
Mn-Nano-ZSM-5	109.9	470	230	0.396
Ni-ZSM-5	124.4	266	46	0.194
Cu-ZSM-5	127.0	273	52	0.198

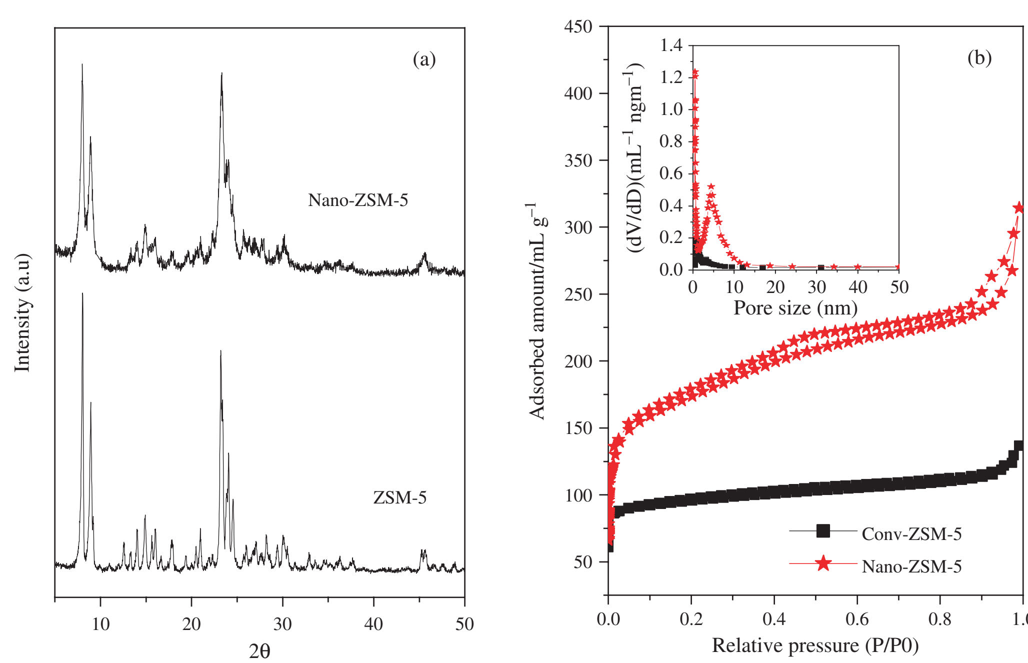

Figure 1. (a) XRD patterns of ZSM-5 and Nano-ZSM-5 and (b) N_2-adsorption isotherms of ZSM-5 and Nano-ZSM-5 (inset shows pore size distribution).

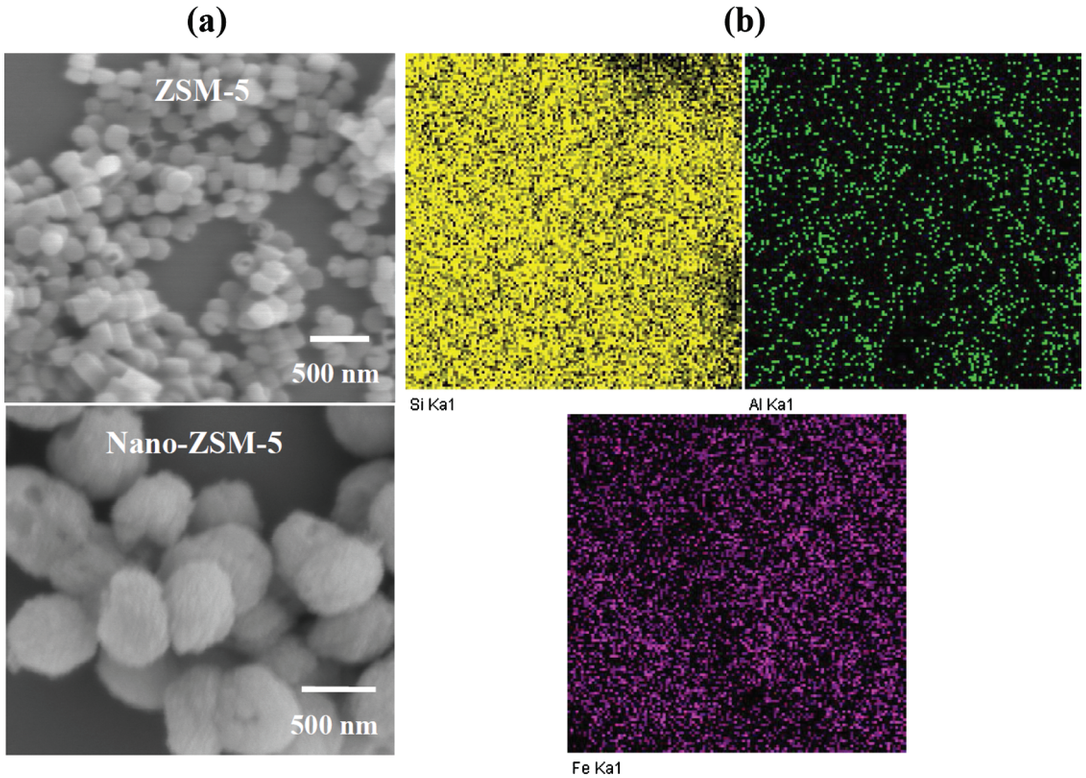

Figure 2. (a) SEM images of ZSM-5 and Nano-ZSM-5 and (b) EDS elemental maps of representative elements in Fe-Nano-ZSM-5.

crystal morphology with large crystal were obtained for ZSM-5 (Fig. 2(a)). Mesopores are created by the crystal packing of zeolite nanocrystals. Mesopore size distribution obtained from N_2-adsorption studies confirms that they are in the range of 2–10 nm. Based on SEM and N_2-adsorption studies, one can conclude that spheroid shaped Nano-ZSM-5 is composed of several nanozeolite particles of approximately 10 nm. EDS mapping confirms the existence of finely dispersed metal species in the Nano-ZSM-5 matrix (Fig. 2(b)). PrTES contains only three hydrolyzable moieties (with one hydrophobic propyl group), which is unfavorable for the formation of extended tetrahedral SiO_2 linkages. Consequently, the zeolite growth is significantly retarded at the organic and inorganic interfaces, resulting in the formation of nanocrystalline zeolites. Mesopores are formed due to the crystal packing of these nanosized zeolite particles. In this study, M-Nano-ZSM-5 and M-ZSM-5 were investigated in the electrochemical oxidation of AA, DA, UA, and Trp. Metal contents obtained from AAS for various transition metal exchanged zeolites investigated in this study were found to be similar (Table I).

3.2. Electrochemical Characterizations of M-Nano-ZSM-5 Modified Electrodes

In this study, electro-catalytic oxidation of AA, DA, UA, and Trp were investigated using M-Nano-ZSM-5 modified electrodes using CV, LSV, and chronoamperometric methods. However, in-depth investigation was made using Fe-Nano-ZSM-5 modified electrode. For comparison, study was also performed using M-ZSM-5 modified electrodes. To explore the electrochemical behavior of the Fe-Nano-ZSM-5 modified electrode, Fe-ZSM-5 modified electrode, and bare glassy carbon electrode, CV was taken in 10 mL buffer solution (pH 3.5). The electrochemical response of Fe-Nano-ZSM-5 modified electrode and Fe-ZSM-5 modified electrode exhibited a pair of well defined redox peaks at 0.29 V and 0.14 V versus Ag/AgCl, and potential peak separation $\Delta E_p = 0.15$ V (Fig. 3), which is attributed to the electron transfer between Fe(II) and Fe(III) in the Fe-Nano-ZSM-5 modified electrode.[22] No redox peak was observed for the bare glassy carbon electrode (Fig. 3). Fe-Nano-ZSM-5 modified electrode exhibits higher current response compared to Fe-ZSM-5 modified electrode.

The influence of the scan rate on the anodic and the cathodic peak currents of Fe-Nano-ZSM-5 modified electrode was studied. CVs at various scan rates (10–600 mV s^{-1}) obtained at the Fe-Nano-ZSM-5 modified electrode show that the anodic and the cathodic peak current increases with the increase in the scan rate (Fig. 4). The plot of the peak currents against the scan rates shows an excellent linear relationship (Fig. 4, inset), suggesting that the electrochemical process is a diffusion-controlled electron transfer process rather than surface controlled at these scan rates.[23] The concentration of electroactive

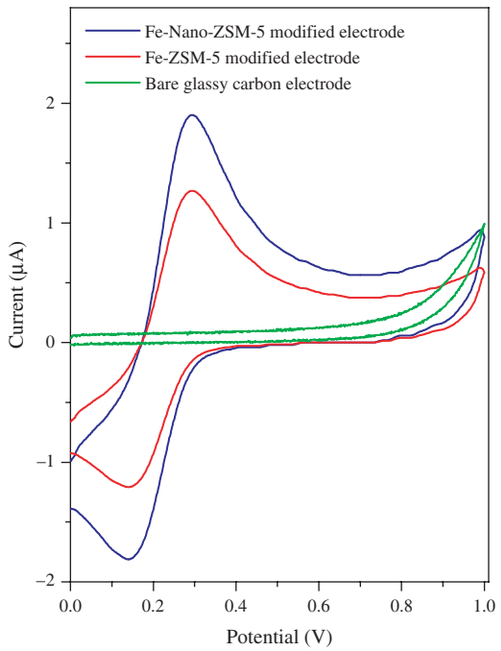

Figure 3. CV responses of Fe-Nano-ZSM-5 modified electrode, Fe-ZSM-5 modified electrode and bare glassy carbon electrode in 10 mL buffer solution (pH 3.5) at a scan rate 50 mV s^{-1}.

species (Γ) can be estimated by plotting the peak currents against the scan rates by following Eq. (1).[23]

$$I_p = n^2F^2A\Gamma\nu/4RT \quad (1)$$

The slope of the anodic peak current against the scan rate is found to be 0.033 (Fig. 4, inset). From the slope of anodic peak currents versus scan rates, the calculated surface concentration of electroactive species in Fe-Nano-ZSM-5 modified electrode is found to be 5.02×10^{-7} mol cm^{-2}. The calculated surface concentrations of electroactive species in Mn-Nano-ZSM-5, Co-Nano-ZSM-5, Ni-Nano-ZSM-5, and Cu-Nano-ZSM-5 modified electrode are found to be 1.7×10^{-7}, 4.7×10^{-7}, 5.3×10^{-7}, and 4.9×10^{-7} mol cm^{-2}, respectively.

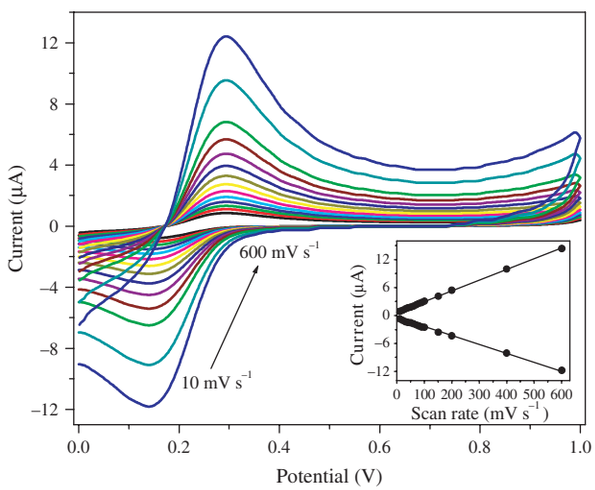

Figure 4. CVs of Fe-Nano-ZSM-5 modified electrode in 10 mL buffer solution (pH 3.5) at various scan rates (10–600 mV s^{-1}). Inset shows plot of peak currents versus scan rates.

Before the determination of AA, DA, UA, and Trp, amperometry was used to evaluate the antifouling property of the Fe-Nano-ZSM-5 modified electrode, since the oxidized products of these analytes could strongly absorb onto the electrode surface that induce electrode fouling and poor reproducibility. The response of the Fe-Nano-ZSM-5 electrode remained quite stable throughout the entire period (40 minutes), with only less current diminutions for the oxidation of AA, DA, UA, and Trp, respectively. Metal ions exchanged on Nano-ZSM-5 matrix catalyze the electrochemical oxidation of AA, DA, UA, and Trp at the electrode surface and the oxidized products of these analytes are diffuse out from electrode surface after the reaction through the inter-crystalline mesopores of zeolite matrix and they are not absorbed at the electrode surface. The synergistic contribution provided by the highly dispersed metal ions (for catalysis) and inter-crystalline mesopores (for enhance diffusion of reactant and product molecules) present in M-Nano-ZSM-5 prevents the electrode from passivation.[21b]

3.3. Individual Electrocatalytic Oxidation of AA, DA, UA, and Trp

The Fe-Nano-ZSM-5 modified electrode was employed to study the electrocatalytic oxidation of AA, DA, UA, and Trp. Prior to the implementation of Fe-Nano-ZSM-5 modified electrode for the oxidation of analytes, a comparison of electrochemical behavior of Fe-Nano-ZSM-5 modified electrode, Fe-ZSM-5 modified electrode, and bare glassy carbon electrode (GCE) towards determination of AA, DA, UA, and Trp individually, was first investigated using CV in 10 mL buffer solution (pH 3.5) (Fig. 5). The results show that analytes are oxidized with well-defined and distinguishable oxidation peaks with peak potentials at 0.19 V, 0.34 V, 0.41 V, and 0.80 V for AA, DA, UA, and Trp, respectively at the Fe-Nano-ZSM-5 modified electrode (Fig. 5(a)). Fe-ZSM-5 modified electrode showed distinguishable oxidation peaks with peak potentials at 0.34 V, 0.41 V, and 0.80 V corresponding to DA, UA, and Trp respectively, but was unable to detect AA (Fig. 5(b)). On the other hand, bare GCE fail to distinguish the oxidation peaks of AA and merged voltammetric anodic peaks appear at 0.36 V, 0.47 V, and 0.81 V for DA, UA, and Trp, respectively (Fig. 5(c)). Compared with the bare GCE, the peak potentials of these analytes at the Fe-Nano-ZSM-5 modified electrode and Fe-ZSM-5 modified electrode are shifted negatively (decrease in oxidation over potential) along with significant increase in oxidation peak current, which indicate that the modified electrode plays a catalytic effect on the oxidation of AA, DA, UA, and Trp. The enlarged separation of the anodic peak potential

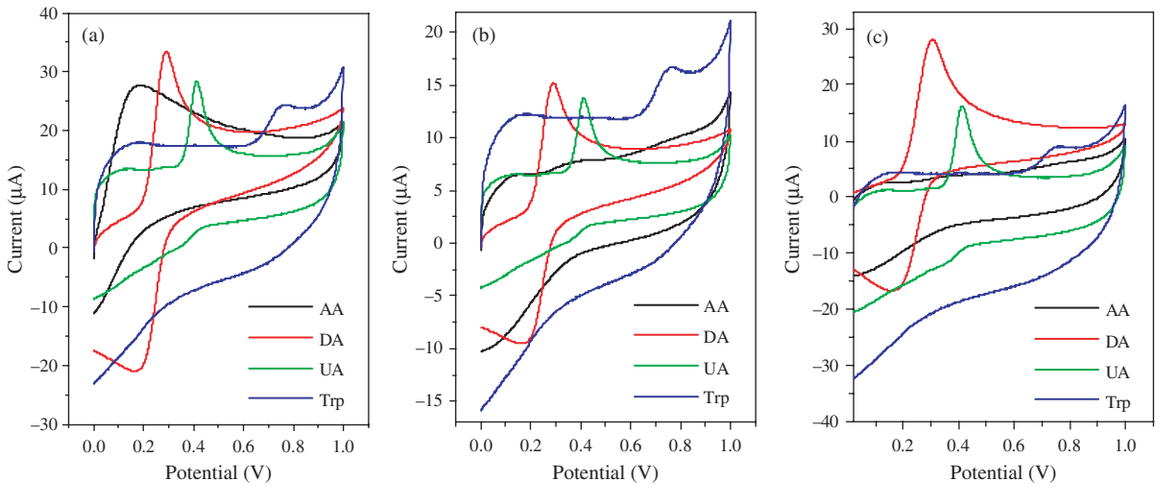

Figure 5. CVs of 10 mL buffer solution (pH 3.5) containing 100 μM each of AA, DA, UA, and Trp at a scan rate of 50 mV s^{-1} at (a) Fe-Nano-ZSM-5 modified electrode, (b) Fe-ZSM-5 modified electrode, and (c) bare glassy carbon electrode.

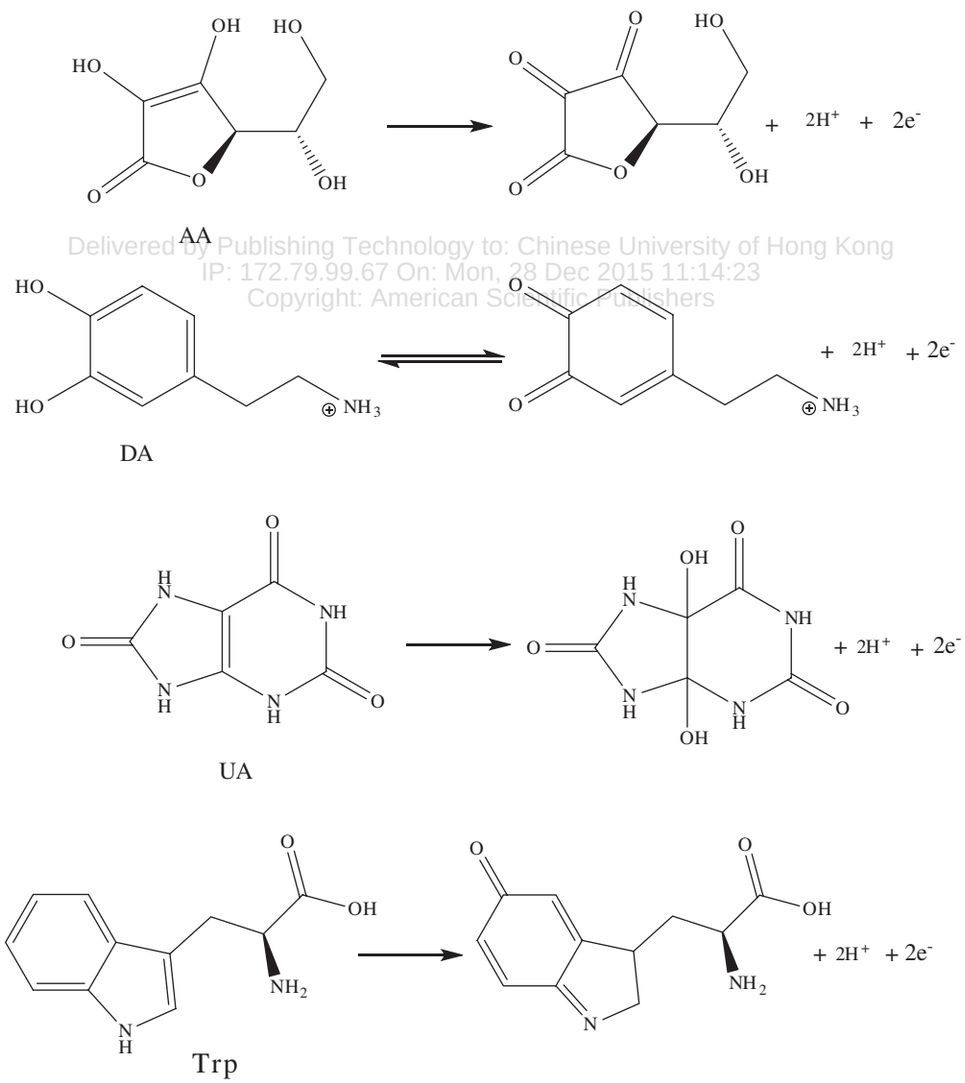

Scheme 1. Electrochemical oxidations of AA, DA, UA, and Trp over ZSM-5 modified electrodes investigated in this study.

coupled with the increased sensitivity makes it possible to effectively determine the individual concentrations of AA, DA, UA, and Trp on Fe-Nano-ZSM-5 modified electrode.

The individual electrocatalytic oxidation of AA, DA, UA, and Trp on the Fe-Nano-ZSM-5 modified electrode was investigated by CV and LSV in 10 mL buffer solution (pH 3.5) at a scan rate of 50 mV s^{-1} by varying their concentrations. In the case of AA, with increase in the concentration of AA, anodic peak current increases, which correspond to the oxidation of hydroxyl groups of the furan ring in AA to carbonyl groups (Scheme 1). No corresponding reduction peak appears, revealing that the oxidation of AA is irreversible. DA undergoes a two-electron oxidation process resulting in the formation of dopamine-o-quinone (DOQ) (Scheme 1). With increase in the concentration of DA, anodic peak current increases, while cathodic peak current decreases, suggesting that the oxidation of DA is reversible. The couple of redox peaks is corresponding to the two-electron oxidation of DA to dopamine-o-quinone (DOQ) and the subsequent reduction of DOQ to DA. With increase in the concentration of UA, anodic peak current increases, which is due to the oxidation of bridging double bond of uric acid to hydroxyl groups (uric acid 4,5 diol) (Scheme 1). Similar enhancement of anodic peak current is also observed for Trp by increasing its concentration, which is due to the oxidation of phenyl ring of Trp (Scheme 1). The modified electrode showed excellent electrocatalytic activity towards AA, DA, UA, and Trp oxidation, individually, in a buffer solution (pH 3.5). The electrochemical response of AA, DA, UA, and Trp increases linearly with the increase in their concentrations. The electrochemical sensor shows a linear response for AA, DA, UA, and Trp in the concentration range of 10 μM to 1 mM.

The diffusion coefficients (D) for these analytes were calculated using chronoamperometry (Fig. 6). Chronoamperograms were obtained at different concentrations of analytes at a desired potential step (250, 400, 550, and 850 mV for AA, DA, UA, and Trp, respectively). The plots of I versus $t^{-1/2}$ exhibited straight lines for different concentrations of analytes. Cottrell equation (Eq. (2)) was used to calculate the diffusion coefficient for various analytes investigated in this study.[24]

$$I_p = nFAD^{1/2}c/\pi^{1/2}t^{1/2} \quad (2)$$

The diffusion coefficients for AA, DA, UA, and Trp, were found to be 21.5×10^{-4}, 15.5×10^{-4}, 3.6×10^{-4}, and 3.8×10^{-4} cm^2 s^{-1}, respectively.

The rate constant for the chemical reaction between the analytes and redox sites of Fe-Nano-ZSM-5 modified electrode was evaluated by chronoamperometry through Eq. (3).[25]

$$I_C/I_L = \pi^{1/2}\gamma^{1/2} = \pi^{1/2}(kC_0t)^{1/2} \quad (3)$$

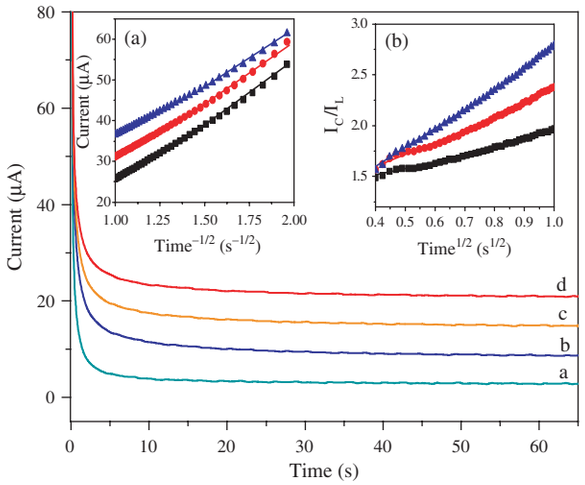

Figure 6. Chronoamperograms obtained at the Fe-Nano-ZSM-5 modified electrode in the absence (a) and in the presence of (b) 100 μM, (c) 200 μM, and (d) 500 μM of AA in 10 mL buffer solution (pH 3.5). Inset: (a) Dependence of current on the time$^{-1/2}$ derived from the chronoamperogram data. (b) Dependence of I_C/I_L on time$^{1/2}$ derived from the data of chronoamperograms.

Based on the slope of I_C/I_L versus $t^{1/2}$ plot; k can be obtained for a given analyte concentration. From the values of the slopes, an average value for k was obtained for the oxidation of analyte. The rate constants for electrocatalytic oxidation of AA, DA, UA, and Trp were found as 2.2×10^2, 3.7×10^3, 1.7×10^3, and 2.6×10^3 M^{-1} s^{-1}, respectively.

For comparison, individual electrocatalytic oxidation of AA, DA, UA, and Trp was also performed on Fe-ZSM-5 modified electrode using CV in buffer solution (pH 3.5) at a scan rate of 50 mV s^{-1}. It may be noted that AA was not possible to detect using Fe-ZSM-5 modified electrode. CV measurements show that for the same concentration of analyte, Fe-Nano-ZSM-5 modified electrode exhibits higher current response compared to Fe-ZSM-5 modified electrode.

3.4. Simultaneous Catalytic Oxidation of AA, DA, UA, and Trp at Fe-Nano-ZSM-5 Modified Electrode

Previous section demonstrated that the Fe-Nano-ZSM-5 modified electrode displayed very good electrochemical catalytic activities towards AA, DA, UA, and Trp oxidation, individually. However, the objective of this study is to determine the concentration of AA, DA, UA, and Trp, simultaneously, from their quaternary mixture. One of such real system is the blood serum, in which all these four species coexist. Following section demonstrates the applicability of Fe-Nano-ZSM-5 modified electrode towards the simultaneous determination of AA, DA, UA, and Trp in their mixture.

For simultaneous determination of AA, DA, UA, and Trp; LSV was carried out at a scan rate of 50 mV s^{-1} in 10 mL buffer solution (pH 3.5) at the Fe-Nano-ZSM-5

modified electrode (Fig. 7). The results show that all four analytes are oxidized with well-defined and distinguishable peaks. An apparent enhancement in the oxidation peak currents was observed, when the concentrations of analytes were increased, indicating that all these analytes has been oxidized at their corresponding potentials by the active Fe-Nano-ZSM-5 modified electrodes via a cyclic mediation redox process. Fe^{2+} is oxidized to Fe^{3+} on the electrode surface at 0.29 V. Fe^{3+} oxidizes the analytes and it undergoes reduction producing Fe^{2+} again. This redox cycle causes an increase in the anodic peak current.[26–28]

Four distinguished anodic peaks at potentials corresponding to the oxidation of AA, DA, UA, and Trp were observed at the Fe-Nano-ZSM-5 modified electrode in the LSV plot during the simultaneous measurement experiments using quaternary mixture having equal concentrations (Fig. 7), which matches well with their individual anodic peak potential as discussed in the above section. LSV studies show that the anodic peak responses for quaternary mixture containing AA, DA, UA, and Trp, are well separated from each other with a potential difference of 140 mV, 120 mV, and 340 mV for the oxidation peak potentials of AA-DA, DA-UA and UA-Trp, respectively, which is large enough to simultaneously determine the concentration of AA, DA, UA, and Trp in their mixture solution. With increase in the concentration of quaternary mixture, the response current corresponding to the analytes oxidation increases. The anodic peak current obtained was found to be linearly dependent on the concentration of analytes (in the range of 10 μM–400 μM for DA, UA, and Trp, whereas 10 μM–300 μM for AA) with the sensitivity of 0.0500, 0.1200, 0.0890, and 0.1000 μA/μM and the lower detection limit of 5.8, 7.2, 3.6, and 5.1 μM for AA, DA, UA, and Trp, respectively (Fig. 7, inset). These results demonstrate that individual or simultaneous determination of these bio-molecules on the Fe-Nano-ZSM-5 modified electrode can be achieved with high sensitivity and selectivity.

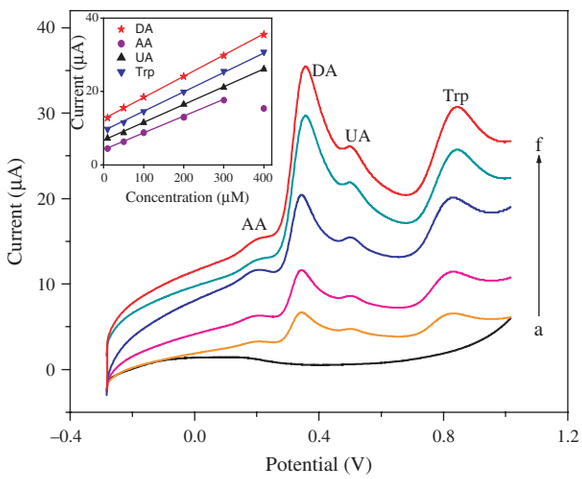

Figure 7. LSVs of the quaternary mixture (having equal concentrations of AA, DA, UA, and Trp) of different concentrations in 10 mL buffer solution (pH 3.5) at Fe-Nano-ZSM-5 modified electrode at a scan rate of 50 mV s^{-1}: (a) blank, (b) 10 μM, (c) 50 μM, (d) 100 μM, (e) 200 μM, and (f) 400 μM. Inset shows calibration curve for the sensor response towards simultaneous electrocatalytic oxidation of AA, DA, UA, and Trp.

Influence of the pH on the simultaneous electrocatalytic oxidation of AA, DA, UA, and Trp was investigated on the Fe-Nano-ZSM-5 modified electrode by varying the pH of the supporting electrolyte (buffer) by LSV at a scan rate of 50 mV s^{-1} in a solution containing equal concentrations of AA, DA, UA, and Trp in a wider pH range (pH 1.0–9.0). The anodic peak current increases by increasing the pH of the medium, with a maximum anodic peak current at pH 3.5 (Fig. 8(a)). This behavior was observed for all bio-molecules investigated in this study. Peak potentials for the oxidation of AA, DA, UA, and Trp shifted negatively with higher pH value, indicating that protons take part in their electrode reaction processes. The maximum separation of peak potentials for AA-DA, UA-DA, Trp-UA is observed at pH 3.5 (Fig. 8(b)). Therefore, in order to obtain high sensitivity and selectivity, pH 3.5 was selected as an optimum pH value for the determination of AA, DA, UA, and Trp in their quaternary mixture. Slope obtained from the linear behavior between the applied potential and the pH for AA, DA, UA, and Trp were found to be 0.063, 0.050, 0.053, and 0.058 V/pH (Eqs. (4)–(7)), which are close to the anticipated Nernstian value (0.059 V/pH) for a two electrons/two protons reaction.[29]

$$\text{Ep (AA)} = -0.063\text{pH} + 0.332 \quad R^2 = 0.995 \qquad (4)$$

$$\text{Ep (DA)} = -0.050\text{pH} + 0.485 \quad R^2 = 0.994 \qquad (5)$$

$$\text{Ep (UA)} = -0.053\text{pH} + 0.650 \quad R^2 = 0.998 \qquad (6)$$

$$\text{Ep (Trp)} = -0.058\text{pH} + 0.919 \quad R^2 = 0.991 \qquad (7)$$

For comparison, simultaneous determination studies were also performed using Fe-ZSM-5 modified electrode by LSV in buffer solution (pH 3.5) at a scan rate of 50 mV s^{-1}. Fe-ZSM-5 modified electrode show the anodic peaks corresponding to DA, UA, and Trp (No AA was detected). LSVs were carried out using Fe-Nano-ZSM-5 and Fe-ZSM-5 modified electrodes in buffer solution (pH 3.5) at a scan rate of 50 mV s^{-1} in the presence and in the absence of analytes (Figs. 9(a), (b)). Oxidation peak currents in the case of Fe-ZSM-5 were found to be less when compared to Fe-Nano-ZSM-5 modified electrode. This improved analytical performance is attributable to highly dispersed Fe^{2+} active centers on Nano-ZSM-5, which facilitates the electron transfer to the electrode. These observations confirm that Fe-Nano-ZSM-5 has high electro-catalytic capability than Fe-ZSM-5 modified electrode. Enhancement of the AA, DA, UA, and Trp oxidation currents at Fe-Nano-ZSM-5 modified electrode can be correlated with the accessibility of more number of Fe^{2+} active centers in the Fe-Nano-ZSM-5 due to its large specific surface area when compared with Fe-ZSM-5.

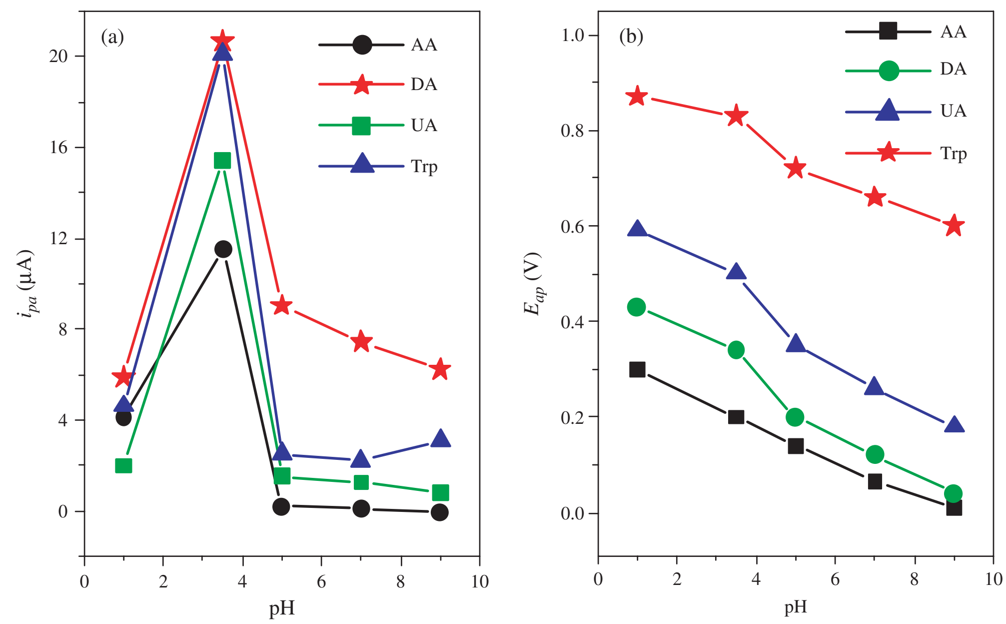

Figure 8. Effect of the pH on (a) the peak current and (b) the peak potential; containing 100 μM each of AA, DA, UA, and Trp at a scan rate 50 mV s^{-1}.

The high electrocatalytic activity of Fe-Nano-ZSM-5 encouraged us to investigate the influence of different M-Nano-ZSM-5 materials towards AA, DA, UA, and Trp oxidation. LSVs were carried out using different M-Nano-ZSM-5 modified electrodes by increasing the concentrations of AA, DA, UA, and Trp in 10 mL buffer solution (pH 3.5) at a scan rate of 50 mV s^{-1}. Although different M-Nano-ZSM-5 modified electrodes exhibited high electrocatalytic oxidation capability for DA, UA, and Trp but they were found to be insensitive towards AA oxidation. A comparison of different M-Nano-ZSM-5 modified electrodes towards the electrocatalytic oxidation of AA, DA, UA, and Trp is summarized (Fig. 10 and Table II). Based on the experimental evidence, one can conclude that Fe-Nano-ZSM-5 exhibited superior sensing ability and current sensitivity compared to other M-Nano-ZSM-5 modified electrodes and Fe-ZSM-5 modified electrode, investigated in this study. High catalytic activity of Fe-Nano-ZSM-5

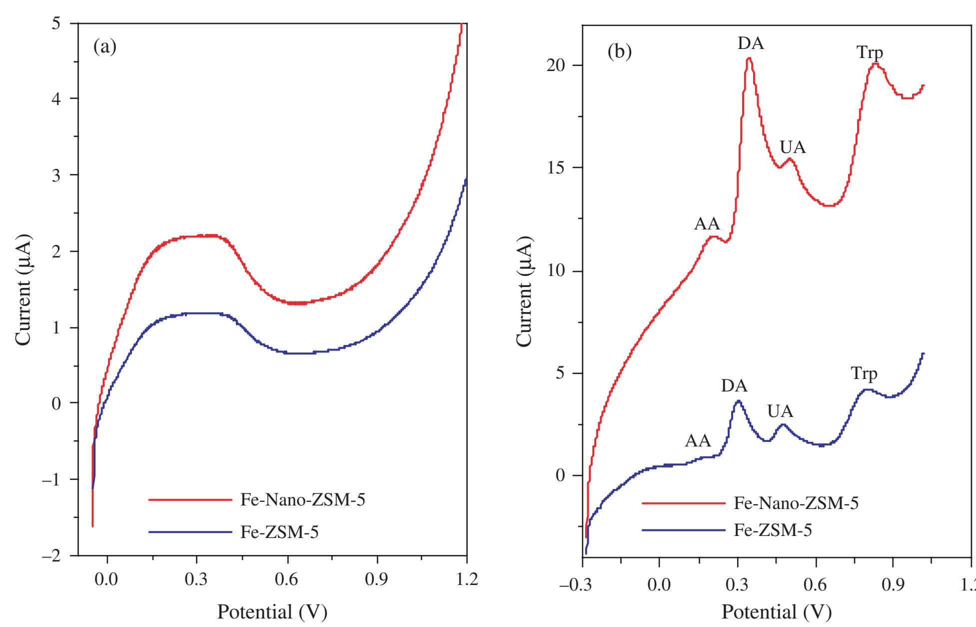

Figure 9. Comparison of LSV of the Fe-Nano-ZSM-5 and Fe-ZSM-5 modified electrodes (a) in the absence and (b) in the presence of AA, DA, UA, and Trp from their quaternary mixture having equal concentration (100 μM) of these analytes in 10 mL buffer solution at a scan rate of 50 mV s^{-1}.

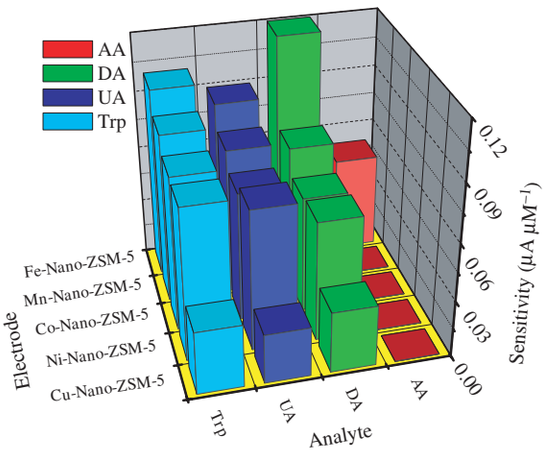

Figure 10. Comparison of the sensitivity for various analytes at different M-Nano-ZSM-5 modified electrodes investigated in this study.

modified electrode towards the oxidation of these analytes may be due the inherent high oxidation capability of Fe^{2+} compared to other M^{2+} in first transition metal atom series and its high electroactive surface concentration. The results obtained using Fe-Nano-ZSM-5 modified electrode for the electrocatalytic oxidation of AA, DA, UA, and Trp were also compared with the previous work reported in the literature and are summarized in Table III.[9–12]

3.5. Reproducibility, Stability, and Anti-Interference Property of the Fe-Nano-ZSM-5 Modified Electrode

The reproducibility and stability of the sensor was evaluated in these sensing studies. Five Fe-Nano-ZSM-5 modified electrodes were made and their current responses to 50 μM concentration of AA, DA, UA, and Trp mixture were investigated. The relative standard deviation (RSD) was found to be 2.5%, confirming that the fabrication method was highly reproducible. The long-term stability of the sensor was evaluated by measuring its sensitivity to 50 μM concentration of AA, DA, UA, and Trp mixture for 20 days. The sensor was stored in refrigerator at 5 °C and its sensitivity was tested at the interval of 5 days. The LSV response of the electrode to the same concentration of AA, DA, UA, and Trp decreased less than 3.5% indicating that the electrode has good reproducibility and excellent stability. In order to investigate the selectivity of the Fe-Nano-ZSM-5 modified electrode towards simultaneous determination of AA, DA, UA, and Trp; LSV measurements were performed in the presence of various interfering agents. The tolerance limit was taken as the maximum concentration of foreign substances that caused a relative error of approximately + 5% for the determination of quaternary mixture containing equimolar concentration (50 μM) of analytes (AA, DA, UA, and Trp) plus the potential interfering substances at pH 3.5. Tolerance limits for Na^+, K^+, Mg^{2+}, Zn^{2+}, and glucose were found to be 250, 200, 200,

Table II. Comparison of the electrocatalytic activities of different M-Nano-ZSM-5 and Fe-ZSM-5 modified electrodes for the simultaneous oxidation of AA, DA, UA, and Trp.

Sample	Electroactive surface concentration (mol cm^{-2})	Analyte	Linear range (μM)	Lower detection limit (μM)	Sensitivity (μA/μM)
Fe-Nano-ZSM-5	5.02×10^{-7}	AA	10–300	5.8	0.0500
		DA	10–400	7.2	0.1200
		UA	10–400	3.6	0.0890
		Trp	10–400	5.1	0.1000
Mn-Nano-ZSM-5	1.67×10^{-7}	AA	0	–	–
		DA	10–300	8.3	0.0740
		UA	10–300	5.9	0.0770
		Trp	10–400	3.4	0.0890
Co-Nano-ZSM-5	4.7×10^{-7}	AA	0	–	–
		DA	10–300	6.3	0.0610
		UA	10–300	3.9	0.0680
		Trp	10–400	6.7	0.0810
Ni-Nano-ZSM-5	5.3×10^{-7}	AA	0	–	–
		DA	10–300	2.2	0.0630
		UA	10–300	5.4	0.0740
		Trp	10–400	2.3	0.0800
Cu-Nano-ZSM-5	4.9×10^{-7}	AA	0	–	–
		DA	10–100	2.1	0.0320
		UA	10–100	5.5	0.0260
		Trp	10–100	3.2	0.0330
Fe-ZSM-5	–	AA	0	10.0	–
		DA	10–200	9.4	0.0690
		UA	10–200	10.0	0.0660
		Trp	10–200	9.1	0.0780

Table III. Comparison of electrocatalytic activities for the simultaneous oxidation of AA, DA, UA, and Trp using different modified electrodes.

S. no.	Electrochemical sensor	Analyte	Linear range	LOD	pH	Reference
1.	Fe-Nano-ZSM-5 modified electrode	AA	10–300 μM	5.8 μM	3.5	Present work
		DA	10–400 μM	7.2 μM		
		UA	10–400 μM	3.6 μM		
		Trp	10–400 μM	5.1 μM		
2.	MWCNT modified carbon-ceramic electrode	AA	15–800 μM	7.71 μM	4.5	[9a]
		DA	0.50–100 μM	0.31 μM		
		UA	0.55–90 μM	0.42 μM		
3	Lanthanum–MWCNT nanocomposites modified electrode	AA	0.40 μM–0.71 mM	140 nM	6.0	[9b]
		DA	0.04 μM–0.89 mM	13 nM		
		UA	0.04 μM–0.81 mM	15 nM		
		NO_2^-	0.40 μM–0.71 mM	130 nM		
4.	Nitrogen doped graphene modified electrode	AA	5.0–1300 μM	2.2 μM	6.0	[9c]
		DA	0.5–170 μM	0.25 μM		
		UA	0.1–20 μM	0.045 μM		
5.	Chitosan-Graphene modified electrode	AA	50–1200 μM	50 μM	7.0	[10a]
		DA	1.0–24 μM	1.0 μM		
		UA	2.0–45 μM	2.0 μM		
6.	Palladium nanoparticle-loaded carbon nanofibers modified electrode	AA	0.05–4 mM	15 μM	4.5	[10b]
		DA	0.5–160 μM	0.2 μM		
		UA	2–200 μM	0.7 μM		
7.	Helical carbon nanotubes modified electrode	AA	25–1045 μM	0.12 μM	7.4	[10c]
		DA	2.5–10 μM	0.08 μM		
		UA	5–175 μM	0.22 μM		
8.	Gold nanoparticles/overoxidized polyimidazole composite modified glassy carbon electrode	AA	210–1010 μM	2 μM	4	[11]
		DA	5–268 μM	0.08 μM		
		UA	6–486 μM	0.5 μM		
		Trp	3–464 μM	0.7 μM		
9.	Fe-Meso-PANI modified electrode	AA	100–300 μM	6.5 μM	3.5	[12]
		DA	100–300 μM	9.8 μM		
		UA	100–300 μM	5.3 μM		
		Trp	100–300 μM	5.2 μM		

150, and 75 μM, respectively. The relative standard deviations (RSD) with respect to the measurement of peak currents for AA, DA, UA, and Trp in the presence of these interference species were found to be 3.5%, 3.0%, 3.3%, 4.0%, respectively; confirming that no significant interference for these common species occurred.

3.6. Determination of AA, DA, UA, and Trp in Standard Sample and Real Samples

Before exploring the potential applicability of Fe-Nano-ZSM-5 modified electrode for real samples (blood serum and urine), a known concentration of quaternary mixture, having different concentrations of individual species, were analyzed. For example: A quaternary mixture containing AA, DA, UA, and Trp having concentrations 60 μM, 10 μM, 80 μM, and 10 μM was prepared and LSV was performed. Concentration of AA, DA, UA, and Trp based on the anodic peak currents and calibration profile obtained previously (Fig. 7) were found to be approximately identical (58.1, 9.5, 78.4, and 9.3 for AA, DA, UA, and Trp respectively) to the original concentrations taken for the analysis. Having confirmed the concentrations of

Table IV. Determination of AA, DA, UA, and Trp in the blood serum and urine samples.

Sample	Analyte	Spiking (μM)	Detected (μM)[a]	Clinical value (μM)	RSD (%)[a]
Serum 1	AA	60	65.7	–	1.9
	DA	30	30.8	–	2.3
	UA	10	24.6	14.0	2.6
	Trp	10	9.6	–	1.7
Serum 2	AA	70	78.1	–	1.5
	DA	40	39.4	–	1.4
	UA	30	45.7	16.5	1.8
	Trp	60	59.3	–	2.2
Urine 1	AA	–	–	–	–
	DA	–	–	–	–
	UA	–	35.6	36.5	2.5
	Trp	–	–	–	–
Urine 2	AA	–	–	–	–
	DA	–	–	–	–
	UA	–	16.5	15.8	2.4
	Trp	–	–	–	–

Notes: For the analysis of the blood serum, samples were spiked with different levels of the known amount of analytes; [a]Average of three replicates.

various species in the standard quaternary mixture, the scope of Fe-Nano-ZSM-5 modified electrode was extended for real samples. Two different kinds of blood serum and urine samples were analyzed using LSV. The results indicate that Fe-Nano-ZSM-5 modified electrode has a good reliable operational ability (Table IV). The interference of other molecules in the samples for the determination of the AA, DA, UA, and Trp was not found. Therefore, the Fe-Nano-ZSM-5 based sensor provides an economical, simple, and efficient protocol for the simultaneous determination of these compounds in biological and pharmaceutical samples.

4. CONCLUSIONS

In this work, transition metal exchanged nanocrytsalline ZSM-5 modified electrodes were constructed and used in the electrochemical oxidation of four important biomolecules of physiological relevance. Transition metal exchanged nanocrystalline ZSM-5 modified electrode exhibited high electrocatalytic activities towards the oxidation of AA, DA, UA, and Trp by significantly decreasing their oxidation over potentials and enhancing the anodic peak currents. The modification of transition metal exchanged nanocrystalline ZSM-5 not only improves the electrochemical catalytic activities towards the oxidation of AA, DA, UA, and Trp, but also resolves the merged oxidation peaks of AA, DA, UA, and Trp into four well-defined peaks, which is very important for simultaneous determination of these analytes. The results demonstrate that Fe-Nano-ZSM-5 has higher catalytic activities towards the oxidation of AA, DA, UA, and Trp with good stability, sensitivity, and selectivity. High selectivity and good antifouling property encouraged us to use Fe-Nano-ZSM-5 modified electrode for the simultaneous determination of AA, DA, UA, and Trp in human blood serum and UA in urine samples. Highly dispersed metal ions on large surface area Nano-ZSM-5 matrix and inter-crystalline mesopores (for enhance diffusion of reactants and products molecules) are responsible for the high electrocatalytic activity of M-Nano-ZSM-5. The analytical performance of this sensor can also be evaluated for electrochemical detection of other electroactive bio-molecules.

Acknowledgments: Authors thank Department of Science and Technology, New Delhi for financial assistance (DST grant SB/S1/PC-91/2012). Balwinder Kaur is grateful to CSIR, New Delhi for JRF fellowship.

References and Notes

1. G. Chen, J. S. Cheng, and J. N. Ye, Fresenius. *J. Anal. Chem.* 370, 930 (**2001**).
2. M. I. Evgen'ev and I. I. Evgen'eva, *J. Anal. Chem.* 55, 741 (**2000**).
3. C. R. Raj, F. Kitamura, and T. Ohsaka, *Analyst* 9, 1155 (**2002**).
4. G. G. Guilbault, Analytical Uses of Immobilized Enzymes, Marcel Dekker, New York (**1984**).
5. A. H. Liu, I. Honma, and H. S. Zhou, *Biosens. Bioelectron.* 21, 809 (**2005**).
6. J. W. Mo and B. Ogorevc, *Anal. Chem.* 73, 1196 (**2001**).
7. O. Arrigoni and C. D. Tullio, *Biochim. Biophys. Acta* 1569, 1 (**2002**).
8. R. D. O. Neil, *Analyst* 119, 767 (**1994**).
9. (a) B. Habibia and M. H. P. Azar, *Electrochim. Acta* 55, 5492 (**2010**); (b) W. Zhang, R. Yuan, Y. Q. Chai, Y. Zhang, and S. H. Chen, *Sens. Actuat. B: Chem.* 166, 601 (**2012**); (c) Z. H. Sheng, X. Q. Zheng, J. Y. Xu, W. J. Bao, F. B. Wang, and X. H. Xia, *Biosens. Bioelectron.* 34, 125 (**2012**); (d) X. Ying, Z. Hong, W. Zhijiao, L. Xiangjun, H. Yujian, and Y. Zhuobin, *J. Nanosci. Nanotechnol.* 13, 1563 (**2013**).
10. (a) D. Han, T. Han, C. Shan, A. Ivaska, and L. Niu, *Electroanalysis* 22, 2001 (**2010**); (b) J. Huang, Y. Liu, H. Hou, and T. You, *Biosens. Bioelectron.* 24, 632 (**2008**); (c) B. Zhang, D. Huang, X. Xu, G. Alemu, Y. Zhang, F. Zhan, Y. Shen, M. W. B. Zhang, D. Huang, X. Xu, G. Alemu, Y. Zhang, F. Zhan, Y. Shen, and M. Wang, *Electrochim. Acta* 91, 261 (**2013**); (d) S. Mahshid, S. Luo, L. Yang, S. S. Mahshid, M. Askari, A. Dolati, and Q. Cai, *J. Nanosci. Nanotechnol.* 11, 6668 (**2011**); (e) Z. Wu, H. Zhao, Y. Xue, X. Li, Y. He, and Z. Yuan, *J. Nanosci. Nanotechnol.* 11, 1013 (**2011**); (f) S. Mahshid, S. Luo, L. Yang, S. S. Mahshid, M. Askari, A. Dolati, and Q. Cai, *J. Nanosci. Nanotechnol.* 11, 6668 (**2011**).
11. C. Wang, R. Yuan, Y. Chai, S. Chen, F. Hu, and M. Zhang, *Anal. Chim. Acta* 741, 15 (**2012**).
12. M. U. Anu Prathap and R. Srivastava, *Sens. Actuat. B: Chem.* 117, 239 (**2013**).
13. A. Corma, *Chem. Rev.* 97, 2373 (**1997**).
14. J. Eric, D. Davies, and N. Jabeen, *J. Inclusion Phenom. Macrocycl. Chem.* 46, 57 (**2003**).
15. C. S. Cundy and P. A. Cox, *Chem. Rev.* 103, 663 (**2003**).
16. R. Srivastava, N. Iwasa, S. I. Fujita, and M. Arai, Progress in Porous Media Research, Nova Science Publisher, New York (**2009**), p. 1.
17. Y. Tao, H. Kanoh, L. Abrams, and K. Kaneko, *Chem. Rev.* 106, 896 (**2006**).
18. J. Pérez-Ramírez, C. H. Christensen, K. Egeblad, and J. C. Groen, *Chem. Soc. Rev.* 37, 2530 (**2008**).
19. R. Srivastava, N. Iwasa, S. I. Fujita, and M. Arai, *Chem. Eur. J.* 14, 9507 (**2008**).
20. (a) R. Kore, B. Satpati, and R. Srivastava, *Chem. Eur. J.* 17, 14360 (**2011**); (b) R. Kore and R. Srivastava, *RSC Adv.* 2, 10072 (**2012**); (c) R. Kore, R. Sridharkrishna, and R. Srivastava, *RSC Adv.* 3, 1317 (**2013**); (d) R. Kore and R. Srivastava, *Catal. Commun.* 18, 11 (**2012**).
21. (a) D. Gligor, S. F. Balaj, A. Maicaneanu, R. Gropeanu, I. Grosu, L. Muresan, and I. C. Popescu, *Mater. Chem. Phys.* 113, 283 (**2009**); (b) B. Kaur, M. U. Anu Prathap, and R. Srivastava, *ChemPlusChem* 77, 1119 (**2012**).
22. A. J. Bard and L. R. Faulkner, Electrochemical Methods-Fundamentals and Applications, John Wiley and Sons, New York (**2000**).
23. M. Sharp, M. Petersson, and K. Edstrom, *J. Electroanal. Chem.* 95, 123 (**1979**).
24. A. J. Bard and L. R. Faulkner, Electrochemical Methods, Fundamentals and Applications, Wiley, New York (**2001**).
25. Z. Galus, Fundamentals of Electrochemical Analysis, Ellis Horwood, New York (**1976**).
26. M. M. Moawad, *J. Coord. Chem.* 18, 61 (**2002**).
27. J. Wang, Y. Wang, H. Lv, F. Hui, Y. Mu, S. Lu, S. Sha, and Q. E. Wang, *J. Electroanal. Chem.* 594, 59 (**2006**).
28. S. M. MacDonald and S. G. Roscoe, *Electrochim. Acta* 42, 1189 (**1997**).
29. M. Hosseini, M. M. Momeni, and M. Faraji, *J. Appl. Electrochem.* 40, 1421 (**2010**).

Received: 7 March 2013. Accepted: 11 April 2013.